

Quality of Anode. Overview of Problems and Some Methods of their Solution Part 2. Improving the quality of the anode

Shahrai S.G.¹, Sharypov N.A.², Polyakov P.V.³, Kondratiev V.V.⁴ and Karlina A.I.⁵

¹ PhD, Associate Professor, ² Senior Lecturer, ³ PhD, Professor, ⁴ PhD, Head of Department of Innovative Technologies,

⁵ Deputy Head of Department of Innovative Technologies,

^{1,2,3} Siberian Federal University, Svobodnyy Ave, 79, Krasnoyarsk, Krasnoyarskiy kray, Russia.

^{3,4} Irkutsk National Research Technical University, 83, Lermontov street, 664074, Irkutsk, Russia.

¹Scopus ID 55579878000, ⁴Scopus ID 56509486000, ⁵Scopus ID 57189716281

Abstract

Laboratory studies have shown that charging the components of the anode mass increases the rate of wetting and impregnation of dust by the pitch in 2-3 times, as evidenced by the shorter time interval during which the moistened coke was immersed in the pitch melt.

The algorithm for obtaining anode mass according to the proposed technological scheme is the following. The components of coke batch - bunches of different fractional composition from bunkers 2 by metering devices 3 and transport screws 5 are fed to preheater 6 where they are heated to a temperature of 200-220 ° C. Further, the heated components of the coke batch are fed into the mixer 11. Coke dust before entering the mixer 11 by the dispenser 4 from the bunker 1 is fed into the dust preheater 9 where it is also heated to a temperature of 200-220 ° C. Pitch, preheated to a temperature of 200-2400C, is fed into the dispenser 8. Further heated coke dust and pitch enter high-voltage charging units 7, where they acquire electrical charges for 1-3 seconds, pitch-negative, and coke dust-positive. At the same time, the voltage at the electrodes of high-voltage charging stations is in the range of 24000-50000 V DC. Charged in this way, pitch and coke dust also enter mixer 11, where they are mixed for 3-4 minutes with each other and with coke batch. From the mixer 11, the finished anode mass is fed into the extruder 10 to form briquettes. In general, the process of anode preparation takes 4-5 minutes, which is 2 times lower than with "traditional" technology.

The presented technology allows essentially to raise productivity of the manufacture equipment of an anode mass at the expense of time reduction of mixing more than in 2 times. Reducing the mixing time of components reduces the specific electricity consumption for anode production by 20-25 kW / t, taking into account the energy consumption of the high-voltage charging unit. An increase in the degree of impregnation of coke dust with pitch reduces the anode fall-off under the conditions of the active electrolyzer and reduces the yield of coal foam by 5-7 kg / ton of Al. Reducing the yield of coal foam reduces the time of the electrolyzer in the depressurized state by an average of 0.2-0.25 hours during the

day, which reduces the specific fluoride emissions by 0.1-0.2 kg / ton Al.

Keywords: aluminum electrolyzer, anode, carbon, coal foam, consumption, oxidation, protection, method.

INTRODUCTION

Dissolved CO₂ in the electrolyte, moving to the surface of the electrolyte, reacts with both carbon in reaction (1) and with dissolved aluminum and sodium. In the case of a rapid chemical reaction, the rate of the gas dissolution is determined by the step of its removal from the surface of the emerging bubble. This case was considered by V.G. Levich for a single bubble, suspended in a turbulent flow of a liquid, and he also proposed an equation for the diffusion flux [1]:



$$j = D^{0,5} \left(\frac{\rho_l}{\rho_s} \right)^{0,5} \cdot \frac{U^{0,75} a^2 c_0}{L^{0,25} \nu^{0,25}} \quad (2)$$

Where: D is the diffusion coefficient of the substance in the liquid; U is the average velocity of the fluid flow; a is the initial radius of the bubble; c_0 is the saturation concentration; L is the characteristic size of the bubble; ν is the kinematic viscosity coefficient/

With decreasing particle size of coal foam, their apparent density ρ_p increases from 1600 kg / m³ ($d \leq 10 \mu m$) and becomes higher than the electrolyte density (2000 kg / m³). The floating velocity V_{fp} of a spherical particle of diameter ($d \leq 1 \mu m$) in the electrolyte is determined by the Stokes equation:

$$V_{fp} = \frac{q d^2}{18} \cdot \frac{\rho_l - \rho_p}{\mu} \quad (3)$$

Where: μ is the dynamic viscosity of the electrolyte, equal to 3 mPa·s

The bubble rise rate V_{br} (cm / s) depends on their radius r and is determined by three equations [2]:

$$V_{br} = \frac{1}{9} \cdot \frac{\rho_l q r^2}{\mu} \quad (r < 0,8 \text{ mm}) \quad (4)$$

$$V_{br} = 1,35 \left(\frac{\sigma}{\rho_l q} \right)^{0,5} \quad (0,8 < r < 2,5) \quad (5)$$

$$V_{br} = 1,18 \left(\frac{\sigma q}{\rho_l} \right)^{0,5} \quad (r > 2,5 \text{ mm}) \quad (6)$$

The rate of bubble uplift, depending on their size, is 20 - 40 cm / s, which is an order of magnitude higher than the rate of emergence of carbon particles. Approximately at the same speed, carbon particles adhering to the bubble will also surface, because the main amount of foam is on the surface of the electrolyte, then, taking into account the low velocities of the emergence of particles with a diameter of $\leq 100 \mu\text{m}$, it can be concluded that they rise due to flotation. The floating foam, the temperature of which is about 950°C , reacts with the oxygen of the air. The burning of carbon in air is limited by mass transfer [3] and the burning rate of carbon is $\sim 1 \text{ g/cm}^2 \cdot \text{h}$. The rate of oxygen delivery to the carbon particles is affected by the integrity of the cryolite-alumina crust, the wetting of the foam by electrolyte and the speed of the gas pump.

ANODE GASES

Anode gases are heavily diluted with air (up to 1 - 3% by volume of CO_2), however, cryolite-alumina crust prevents air penetration into the space side-anode. This leads to a reduction in the burnout of the foam and the anode. Even in the presence of cracks and holes in the crust (for example, under the feeders), the intake of air under the crust is difficult due to the difference in pressure. The pressure under the crust is approximately on 100 Pa higher than under the shelter shields of the electrolyzer.

In the case of air delivery under the crust, the influence on the access of oxygen to carbon is exerted by wetting of the foam with electrolyte. Depending on the angle of wetting, there are three possible options for the behavior of a carbon particle on the surface of the electrolyte (Fig. 1) [4]:

A) the wetting angle θ is less, b) is equal and c) is greater than 90° .

It is known that near the vertical surfaces of the anode immersed in the melt and under the crust $\theta = 100-110^\circ$, so the foam is poorly wetted by the electrolyte and part of its surface is accessible to the gas (Figure 1c). It should be noted that in cases a) and b) it is also possible to form a thin film of electrolyte on the surface of carbon particles [5].

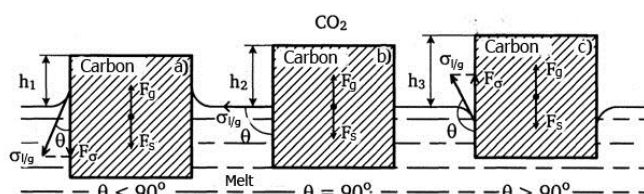


Figure 1: Forces acting on a particle on the surface of the melt

Coal foam accumulates beneath the feed points of the bath with alumina, and can adversely affect the solubility of alumina, since instead of dispersing alumina, clumps are formed in the melt that are difficult to penetrate into the melt. The poor solubility of alumina is the reason for the formation of sediments on the bottom, the occurrence of anode effects, and an increase in the temperature of the electrolyte. The concentration of alumina in the bath plays a decisive role. Local depletion of the concentration may lead to a local anode effect.

The situation of increasing the resistance of the electrolyte due to the accumulating foam is equivalent to the bubble resistance in the bath, which is proportional to the volume of the gas-containing layer of the electrolyte. The increase in the resistance of the bath is proportional to the volume fraction of carbon in the melt. If the content of the foam in the electrolyte is 5% by weight, in order to compensate for its resistance, a 2 mm reduction in IPD (inter-pole distance) is necessary. By experimental measurements it was established that, with a highly-foamed electrolyte, the baths work with IPD, reduced by 4-6 mm. Many automatic process control systems (ACSSs) in this case reduce the voltage on the bath, which is accompanied by a further decrease in IPD. Decrease in IPD affects the stability and productivity of the bath, which increases the formation of foam, forming a closed circle, shown in Fig. 2 [6].



Figure 2: A vicious circle created by coal foam

During the replacement of the anode, the foam floats to the surface of the melt. Because of intense radiation of heat by a black body, the electrolyte particles in the pocket crystallize, and the cold anode completes their freezing. At the same time, the thickness of the frozen electrolyte layer adhered to the anode bottom reaches 2 to 3 cm. This causes the effect of reducing IPD and reducing the melting rate of the adhered layer, due to the following reasons:

- the need for a higher temperature to melt the electrolyte containing coal particles;

- reduction of the contact area of the anode with the electrolyte;
- low overheating of the electrolyte under the anode, which suppresses melting of the adhered layer.

Thus, there is a high risk of further sticking of carbon particles and electrolyte and formation of a cone at the anode (Figure 3), causing a short circuit with cathode aluminum. More than 60% of the current of the entire anode flows through the cone, and the current loss can reach 3%, depending on the number of anodes and the duration of the short circuit. For example, for electrolytic cells equipped with 20 anodes, 10% of which are short-circuited with an average duration of 6 days, the permanent current loss is 1.5%.

With stable parameters of electrolysis, the formation of foam is a consequence of the low quality of the anode. In combination with technological disruptions, a high level of foam can lead to a crisis that reduces production performance for a long period.

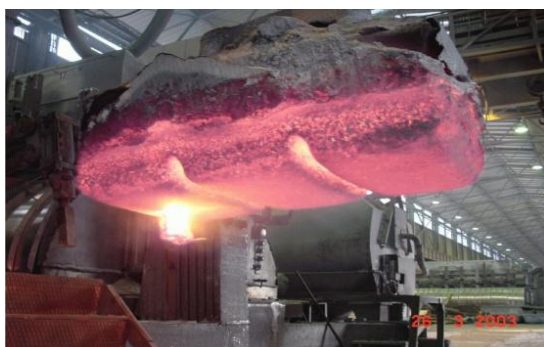


Figure 3: Anode cone at the base of the anode

Effect of additives on the reactivity of the anode

The effect of additions of Na_2CO_3 , ZnS and Al_2O_3 on the reactivity and consumption of the anode in conditions of increasing the content of sulfur cokes and metallic impurities was considered in [7].

The reactivity of anodes with additions of Na_2CO_3 , ZnS and Al_2O_3 as an independent sulfur source or in combination with Na_2CO_3 was studied in the following way. The anode carbon materials used in this study were obtained by drilling out cores from full-scale fired anodes, or from small-scale laboratory blocks sealed with vibration and fired at 1265°C . Samples drilled from industrial anodes were used to study the effect of Na_2CO_3 and ZnS additives, while samples from laboratory blocks were used to study the effect of the Al_2O_3 additive.

Na_2CO_3 was introduced into the sample by immersion in soda solutions of various concentrations for a certain time. After soaking, the samples were dried at 150°C for 15 hours, cooled in a desiccator and weighed. This drying period was enough to get rid of all the water. The Na_2CO_3 content in the sample was determined by increasing its weight.

Due to the fact that ZnS is insoluble in water, its addition to the sample by the impregnation method is impossible. Therefore, for the tests, samples of anodes were prepared with the addition of specified amounts of finely divided Na_2CO_3 and ZnS .

The reactivity of carbon materials was determined by the usual method described in [8; 9; 10]. Samples were exposed to a continuous stream of CO or air for 2 to 4 hours at a constant temperature. Samples with a diameter of 20 mm and a height of 40 mm were suspended in an oven equipped with electronic scales, which allowed a continuous recording of the sample weight. The reaction capacity of the sample in CO_2 was studied at a temperature of $948 \pm 3^\circ\text{C}$, in air at $530 \pm 2^\circ\text{C}$.

The consumption of the anode material with the addition of Al_2O_3 was studied in a laboratory electrolytic cell equipped with an anode gas collection system ($\text{CO} + \text{CO}_2$). Anodes with a diameter of 42 mm for 3 hours were subjected to electrolysis at a constant current of 13 A and a temperature of $980 \pm 2^\circ\text{C}$ in a cryolite containing 7% by weight of AlF_3 and 5% by weight of CaF_2 , which was saturated with alumina and used as an electrolyte. The experimental conditions were strictly the same for all experiments.

The effect of the addition of Na_2CO_3 on the oxidation of anode samples in air and in CO_2 is shown in Figure 4.

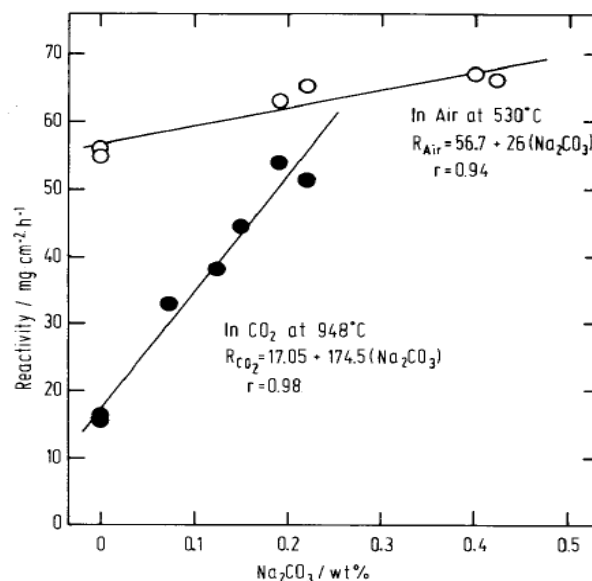


Figure 4: Effect of Na_2CO_3 on the reactivity of the anode in air and CO_2

It can be seen from the graph that Na_2CO_3 catalyzes both reactions. While the effect of the additive on oxidation in air is small, in a CO_2 environment the catalytic effect is almost 7 times stronger.

In Figure 5, the reactivity data are expressed as a function of the total sodium concentration, by adding it with the introduced Na_2CO_3 . This figure shows the data obtained in

[13], where the anode samples were made from raw materials with different sodium content. The data obtained in both cases show an extremely high sensitivity of the anode to oxidation in CO₂ in the presence of sodium, regardless of the content of other metallic impurities. It is believed that the large difference in the catalytic effect of Na₂CO₃ on the reactivity of the anode in CO₂ and in air is due to the different behavior of sodium carbonate at these temperatures during both reactions. In the works [11; 12] Such a behavior of Na₂CO₃ is due to its thermal dissociation.

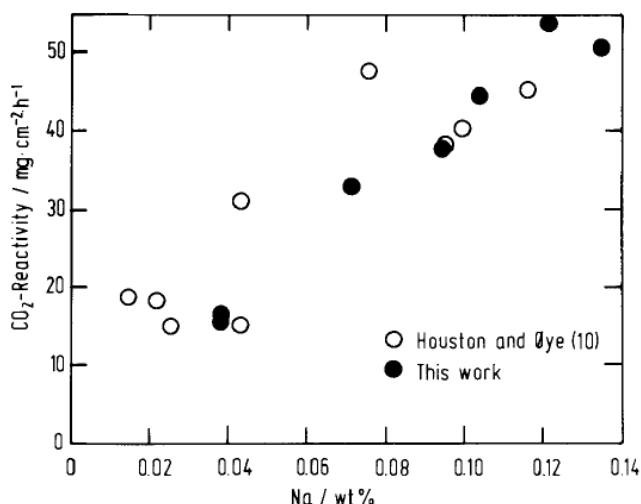
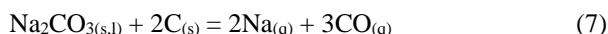
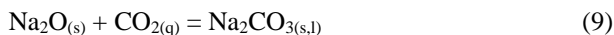
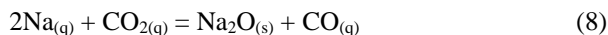


Figure 5: Reactivity of the anode in a current with CO₂ as a function of the sodium content

Due to the high temperature, the following reaction is possible:



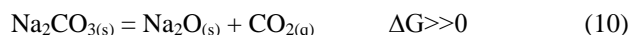
The equilibrium constant for this reaction at 927 °C is $\sim 4 \cdot 10^{-7}$, which can cause a significant increase in the vapor pressure of Na, with decreasing CO pressure. The separation of sodium vapor during the catalytic oxidation of graphite in CO₂ at 1000 °C was indeed noted in [17]. Since sodium vapor has a high reactivity, their formation can lead to the following reactions:



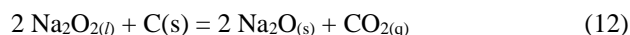
Moreover, at the temperature under consideration, both reactions are thermodynamically possible.

In the case of the oxidation reaction of the anode in air, due to a decrease in temperature < 600 °C, the sodium vapor pressure, in accordance with reaction (7), will be insignificant, since the equilibrium constant of reaction (7) is $\approx 4 \cdot 10^{-24}$ at

527 °C, and at this temperature, the dissociation of Na₂CO₃, according to the reaction (4), will be very weak:



Nevertheless, according to [17], the dissociation of sodium carbonate in the presence of carbon and oxygen is enhanced as a result of the following successive reactions:



Which can explain the weak catalytic effect.

The effect of the addition of ZnS with and without the use of Na₂CO₃ is shown in Figure 6.

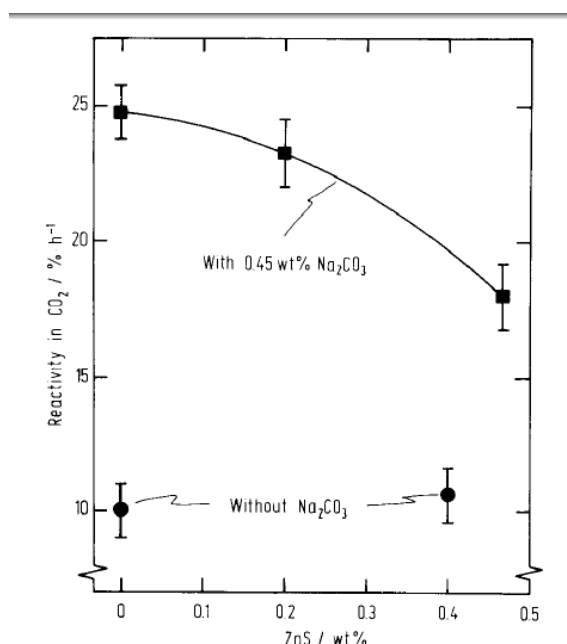
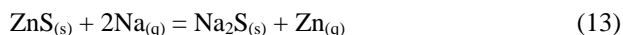


Figure 6: Effect of ZnS on the reactivity of the anode in the current of CO₂ in the absence of Na₂CO₃ and the addition of 0.45% by weight of Na₂CO₃

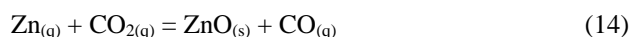
Figure 6 shows that the addition of ZnS only to 0.40% by weight does not cause significant changes in reactivity in the current of CO₂, and the loss of reactivity of carbon is 10-11%, which can be attributed to the experimental error. Addition of 0.45% by weight of Na₂CO₃, as expected, increases the reactivity loss to 25%, in the absence of ZnS.

An interesting feature of the experiment was the fact that the amount of Na₂CO₃ in the samples was maintained at a constant level of 0.45% by weight, while the content of the ZnS additive was increased from 0 to 0.47% by weight, which resulted in a decrease in the reactivity of the anode in CO₂ from 25 to 18%. In other words, the catalytic effect of Na₂CO₃ decreases with increasing S / Na ratio in the sample. The reason for this behavior is probably the presence of additional chemical equilibrium, which can be expressed as follows:



As indicated earlier, the sodium vapor pressure is again formed by reaction (7) due to the dissociation of Na_2CO_3 . However, in the second stage of the catalytic cycle, reaction (8) competes with reaction (13). From the thermodynamic point of view, the Gibbs energy of reaction (13) is $\Delta G = -136.8$ kJ, and the reaction (7) $\Delta G = -67.8$ kJ at 927°C . Therefore, it is reasonable to assume that at least a portion of the sodium vapor is converted to Na_2S , and thus the amount of free sodium for the catalytic cycle decreases.

The vapor of zinc, formed as a result of reaction (13), is usually oxidized to ZnO :



As indicated above, ZnO is not active with respect to oxidation of the anode in CO_2 , and Na_2S is a very stable compound, hardly active as a catalyst for reactivity. Thus, reaction (13) is considered to be an obstacle to the observed catalytic effect produced by Na_2CO_3 .

In the light of the foregoing, it is possible to use a similar interaction of sodium and sulfur in the compositions of industrial anodes. Petroleum coke with a high sulfur content may have a positive effect on reducing the reactivity of the anode in a current of CO_2 by suppressing the catalytic ability of sodium. This may cause disagreement with previously published data on the effect of sulfur on the oxidation of the anode in CO_2 .

The effect of the addition of Al_2O_3 on the physical properties of the anode is shown in Table. 1.

Table I. Some Physical Properties of the Anode Blocks Containing Al_2O_3 as additive

Al_2O_3 content (wt%)	Apparent Density (g cm^{-3})	Cumulative Pore Volume ($\text{cm}^3 \text{g}^{-1}$)	Total Poro-sity (%)	Electrical Resistivity ($\mu\Omega\text{m}$)	Thermal Conductivity ($\text{Wm}^{-1} \text{K}^{-1}$)
0	1.53	0.156	23.6	62.2 ± 1.4	3.99 ± 0.03
1	1.50	—	—	66.4 ± 1.1	—
2	1.52	0.157	23.9	—	3.94 ± 0.04
3	1.51	—	—	60.3 ± 2.0	—
5	1.55	0.153	23.7	65.8 ± 0.6	3.80 ± 0.04

The apparent density and porosity of the anodes with the addition of Al_2O_3 remain unchanged, as is the pore size distribution, as illustrated in Figure 7 for "pure" anode samples and samples with an additive of 5% by weight of Al_2O_3 .

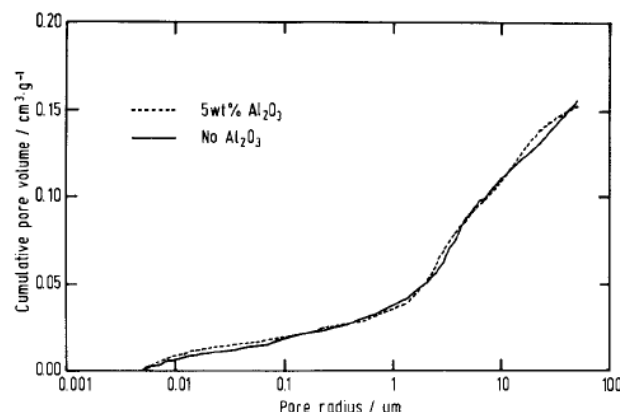


Figure 7: Typical pore spectra of anode samples without the addition of Al_2O_3 and with the addition of 5% by weight of Al_2O_3

The correlation between the resistivity of the anode and the content of Al_2O_3 is not observed, and the thermal conductivity decreases almost in proportion to the increase in the Al_2O_3 addition.

Reactivity of anode samples with an additive of 5% by weight of Al_2O_3 is shown in Figure 8.

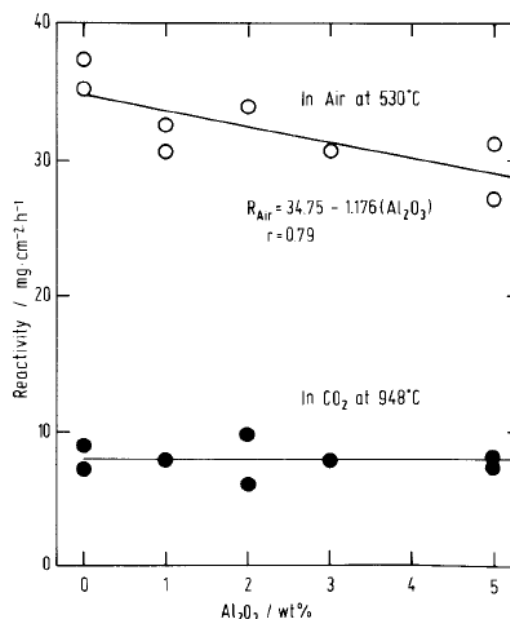


Figure 8: Effect of Al_2O_3 on the reactivity of the anode in air and CO_2

While the reactivity in air linearly decreases with increasing Al_2O_3 content, the reactivity in the current of CO_2 remains at the same level, at any content of aluminum oxide. This different behavior of the anode samples in air and in CO_2 is believed to be due to the temperature difference at which these reactions were studied.

From the technological point of view, the reduction in oxidizability in air is very useful, since the consumption of the anode decreases. Another useful aspect is a decrease in thermal conductivity with the addition of Al_2O_3 , which will reduce the temperature of the anode in the industrial cell. According to [13], a decrease in thermal conductivity of $0.1 \text{ W}^{-1}\text{K}^{-1}$ reduces the anode surface temperature by 2.75°C . Even such a small decrease in temperature in the upper part of the anode will lead to significant savings in the carbon material, since its reactivity in air depends strongly on temperature. This combined effect makes the addition of Al_2O_3 to industrial anodes attractive.

The effect of the addition of Al_2O_3 on the anode consumption

The effect of the addition of Al_2O_3 on the anode consumption in the laboratory cell is shown in Figure 9.

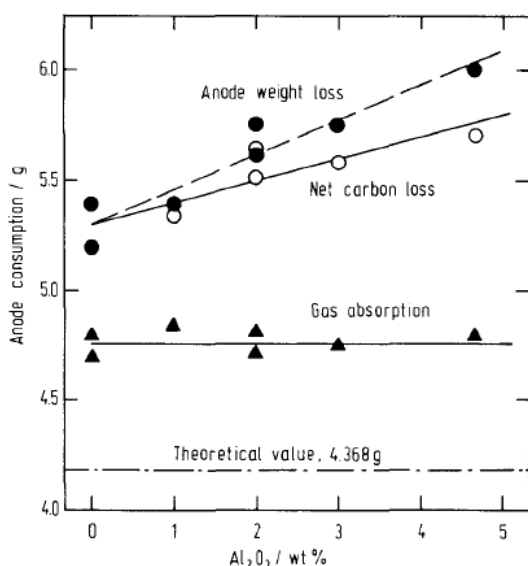


Figure 9: Effect of Al_2O_3 on the anode consumption after electrolysis at 980°C and 13 A, for 3 hours. The anode consumption is determined by the loss of its weight minus the Al_2O_3 dissolved in the melt

The theoretical anode consumption corresponds to its 100% oxidation in CO_2 . It is seen that with an increase in the Al_2O_3 content, the anode is consumed at a faster rate. Nevertheless, some of these losses are caused by the dissolution of Al_2O_3 in the electrolyte.

Anode weight loss correction for the corresponding Al_2O_3 content gives a net carbon consumption, which also increases with the addition of alumina. These data are presented in Figure 10. Oxidability of the anode does not cause an increase in the anode flow rate and this agrees with the results of the tests for the determination of the reactivity in the CO_2 current.

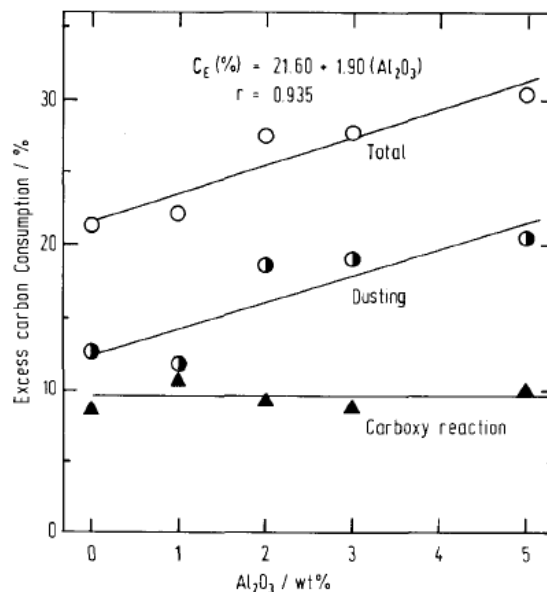


Figure 10: Dependence of excess carbon consumption on the content in the anode of Al_2O_3

To a higher consumption of carbon material leads the formation and removal of coal foam. In accordance with Figure 10, the most optimal is the addition of Al_2O_3 in an amount of 1.9% by weight.

Summarizing the results obtained, the authors of [14] draw the following conclusions:

- Na_2CO_3 acts as a strong catalyst for reactivity, while its effect on the rate of carbon oxidation in air is very modest;
- ZnS is not active for reactivity, nevertheless it has the ability to significantly reduce the catalytic ability of sodium, especially in the presence of Na_2CO_3 ;
- Al_2O_3 does not affect the reactivity in CO_2 , but reduces the reactivity in air.

It was established in [15] that V and Ni are catalysts for oxidation of the anode in air. The same is true for Na and Fe if we consider the reactivity of the anode in CO_2 . However, it is often difficult to separate the effect of different elements due to the joint presence of other impurities. An example of this is the presence of sulfur, about which contradictory results were reported in the work.

Additives AlF_3 , B_2O_3 , SiO_2 and phosphorus-containing compounds were tested as inhibitors of anode oxidation [9]. However, only a few published data about the effect of Al_2O_3 on the reactivity and anode carbon consumption. It was reported in [16] that Al_2O_3 catalyses the oxidation of graphite in air. A significant increase in the consumption of Soderberg test anodes containing Al_2O_3 as an additive was reported in [17]. In the works [18; 19] as an alternative to the traditional, composite anodes containing from 20 to 85% by weight of Al_2O_3 were proposed, while in [13] there is a minimum

oxidation of such an anode by air, apparently due to a decrease in the fraction of carbon in it.

Proposed measures to reduce the consumption of pure carbon and the yield of coal foam.

According to [20], the surface area available for reaction (7) depends on the properties of the pitch and the depth of its penetration into the pores of the coke-filler. When coke is impregnated, the maximum capillary rise height h_{max} is determined by the surface tension (σ) of the liquid phase, the wetting contact angle ($\cos \theta$) and the density ρ_l and can be determined from the expression:

$$h_{max} = \frac{2\sigma_{lg}\cos\theta}{r\rho_l g} \quad (15)$$

According to [21], the Maximum lifting height of the pitch along the capillaries depends on its softening temperature and reaches 7 mm. The most rapid lifting height of the pitch in the capillaries varies in the temperature range 150 - 175 ° C. A further increase in temperature to 200 ° C does not lead to a noticeable change in the lifting height of the pitches in the capillaries.

Increase lifting height of the pitch in coke capillaries, and thus reduce the consumption of the binder is proposed through the use of a sound capillary effect, when ultrasound causes an abnormally deep penetration of liquid into capillaries and narrow slits. In this case, the height of the lifting and the depth of penetration significantly exceed the corresponding values, caused only by the surface tension of the liquid pitch [22]. The use of a sound-capillary effect will ensure an improvement in the quality of the anode mass with a lower pitch consumption, which will have a favorable effect on the environmental performance of both the anode production and aluminum production in general.

Another way to increase the degree of impregnation by pitch is to impart a multi-polar electrical charge of coke dust and pitch using a high-voltage DC charging unit that provides a voltage on the electrodes from 24 to 50 thousand volts. In this case, the pitch is given a negative charge, the coke dust is positive [23].

Laboratory studies have shown that charging the components of the anode mass increases the rate of wetting and impregnation of dust by the pitch in 2-3 times, as evidenced by the shorter time interval during which the moistened coke was immersed in the pitch melt (Figures 11-16) [24].



Figure 11: Without giving charge to AM components, the initial state



Figure 12: With the charged the AM components, the initial state



Figure 13: Without charging the AM components after 50 seconds

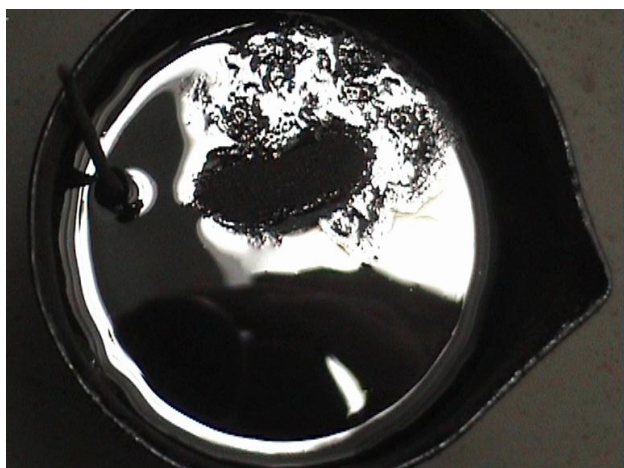


Figure 14: With charged the AM components in 50 seconds



Figure 15: Without charging the AM components after 5 minutes

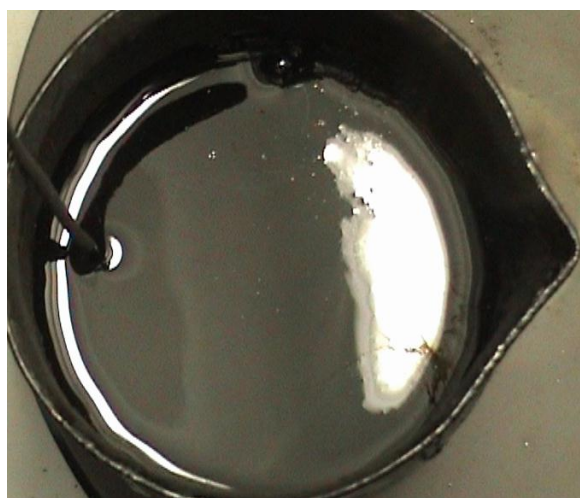


Figure 16: With charged the AM components in 3 minutes

The technology of charging components of pitch and coke with multi-polar charges can be easily adapted to the existing technological process of obtaining anode mass. In this case, a high-voltage dust charging installation is located between the coke dust preheater and the mixer, pitch - between the pitch meter and the mixer (Figure 17).

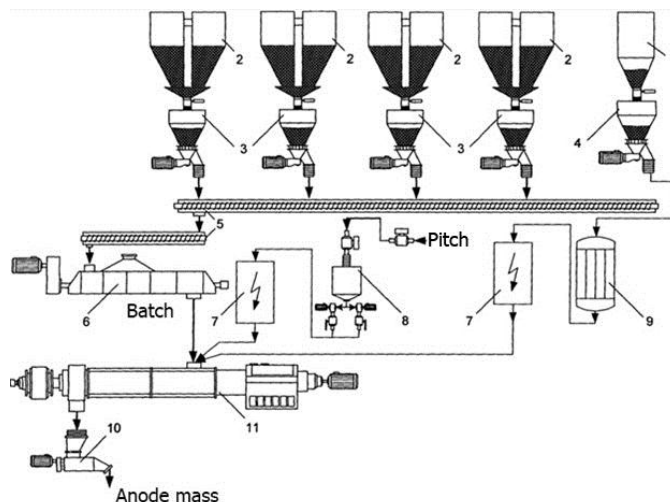


Figure 17: Technological scheme for obtaining anode mass with a high-voltage charging installation: 1,2 – bunkers of dust and coke bunches; 3,4 – dosing equipment for dust and coke bunches; 5 – auger conveyor; 6 – charge heater; 7 – high-voltage charging installations of coke dust and pitch; 8 – pitch dispenser; 9 – dust preheater; 10 – extruder; 11 – mixer

The algorithm for obtaining anode mass according to the proposed technological scheme is the following. The components of coke batch - bunches of different fractional composition from bunkers 2 by metering devices 3 and transport screws 5 are fed to preheater 6 where they are heated to a temperature of 200-220 ° C. Further, the heated components of the coke batch are fed into the mixer 11. Coke dust before entering the mixer 11 by the dispenser 4 from the bunker 1 is fed into the dust preheater 9 where it is also heated to a temperature of 200-220 ° C. Pitch, preheated to a temperature of 200-2400C, is fed into the dispenser 8. Further heated coke dust and pitch enter high-voltage charging units 7, where they acquire electrical charges for 1-3 seconds, pitch-negative, and coke dust-positive. At the same time, the voltage at the electrodes of high-voltage charging stations is in the range of 24000-50000 V DC. Charged in this way, pitch and coke dust also enter mixer 11, where they are mixed for 3-4 minutes with each other and with coke batch. From the mixer 11, the finished anode mass is fed into the extruder 10 to form briquettes. In general, the process of anode preparation takes 4-5 minutes, which is 2 times lower than with "traditional" technology [25-33].

The presented technology allows essentially to raise productivity of the manufacture equipment of an anode mass at the expense of time reduction of mixing more than in 2

times. Reducing the mixing time of components reduces the specific electricity consumption for anode production by 20-25 kW / t, taking into account the energy consumption of the high-voltage charging unit. An increase in the degree of impregnation of coke dust with pitch reduces the anode fall-off under the conditions of the active electrolyzer and reduces the yield of coal foam by 5-7 kg / ton of Al. Reducing the yield of coal foam reduces the time of the electrolyzer in the depressurized state by an average of 0.2-0.25 hours during the day, which reduces the specific fluoride emissions by 0.1-0.2 kg / ton Al.

According to [25], oxidation of the anode occurs over all its surfaces, as shown in Figure 18

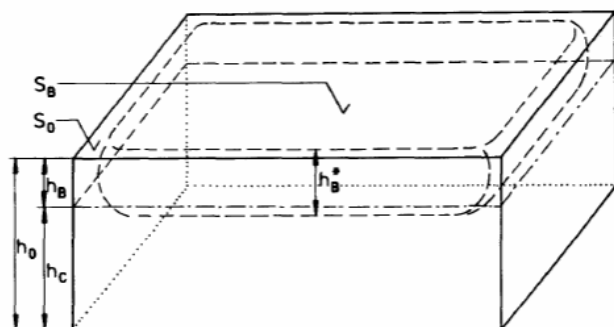


Figure 18: Dimensions and contour of the anode and anode cinder

To reduce the oxidation of the side surface of the anode is proposed by means of a device on its side, facing the flange sheet of the cathode device of the electrolyzer of the notch-shelf, as shown in Figure 19 [26].

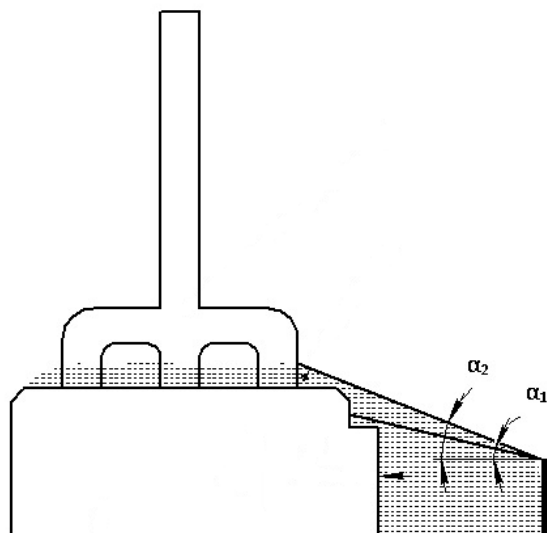


Figure 19: Annealed anode with a notch on the side surface

With this anode configuration, the loading of the covering material is carried out in two stages. The first layer of the

covering material is loaded onto the notch-shelf, forming an angle α_1 between the upper boundary of the covering material and a horizontal plane within the range of $37 - 42^\circ$, which corresponds to its angle of repose. Further; after sintering of the covering material and formation of a firm crust on its surface, a second layer of covering material is loaded onto it, forming an angle α_2 between the upper boundary of the covering material and a horizontal plane in the range $55-60^\circ$. Thus, the efficiency of protecting the front side of the baked anode from air oxidation is increased, its mass is reduced, and also the anode cinder, involved in the recycling of the anodes.

Increase the stability of the upper surface of the anode to oxidation by air is proposed by changing the algorithm for loading the cover material onto it. Initially, a layer of cryolite-alumina batch with a thickness of 5-10 cm is loaded onto the anode surface. Then, after 1-1.5 hours, an alumina layer 3-5 cm thick is loaded onto the crust of the sintered cryolite-alumina batch [27, 34-37]. When loading the cryolite-alumina batch on the surface of the anode massif, the alumina entering it is impregnated with electrolyte vapors, and the fluoride salts begin to melt when heated to 700°C , thus forming a strong crust with low gas permeability, from 0.02 to 0.04 NPM. However, the thermal conductivity of the crust can reach 1.5-1.6 W / m · K, which is accompanied with high losses of the heat by the electrolyzer. A decrease in these losses is ensured by an alumina layer whose thermal conductivity is $\sim 0.14\text{ W / m} \cdot \text{K}$.

ACKNOWLEDGEMENT

This paper has been prepared with financial support from the Ministry for Education and Science of Russian Federation (Order No.218 adopted on the 9th of April 2010 by the Government of the Russian Federation.) within the framework of the project 02.G25.31.0181 "Development of heavy duty energy efficient technology for aluminum RA-550" in the framework of realization of complex projects in high-tech production, approved by the RF Government decree № 218 from April 9, 2010.

REFERENCES

- [1] Levich, V.G. Fiziko-himicheskaja gidrodinamika. – M.: Fizmatgiz, 1959. – 700s.21.
- [2] Burnakin V.V. Hidro- gazodinamika i massobmen v jelektrometallurgii aljuminija i magnija: diss....dokt. tehn. nauk: 05.16.03 / Burnakin Vitalij Viktorovich. – Krasnojarsk, 1990. – 330 s.
- [3] Grjotheim, K. Aluminium Smelter Technology / K. Grjotheim, B.J. Welch. – Düsseldorf: Aluminium – Verlag, 1988. – 327 p.
- [4] Vinogradov A.M., Poljakov P.V., Mihalev Ju.G. i [dr.]. Povedenie ugleroda i karbida aljuminija v

- jelektrolitah promyshlennyh vann / Sb. dokl. II Mezhd. kongr. Cvetnye metally – 2010, pp. 515-522.
- [5] Chizmadzhev, Ju.A., Markin, V.S., Tarasevich, M.R. i [dr.]. Makrokinetika processov v poristyyh sredah (toplivnye jelementy) .- M.: Nauka, 1971. – 364 s.
- [6] Tarcy G. P., Tørklep K., Current efficiency in prebake and Søderberg cells, *Light Metals* 2005, pp 319-324.
- [7] Halldor Gudmundsson. Anode dusting from a potroom perspective at Nordural and correlation with anode properties / *Light Metals*, 2011, pp. 657 -662.
- [8] P.J. Rhedey. "Carbon Reactivity and Aluminium Reduction Cell Anodes", *Light Metals* 1982 (Warrendale, PA: TMS-AIME) pp. 713-725.
- [9] S.R. Brandtzaeg, "Structural Changes During Calcination of Coke and Anthracite", (Dr.ing. thesis, Norwegian Inst. of Technology 1985).
- [10] G.J. Houston and H.A. Oye, "Reactivity Testing of Anode Carbon Materials", *Light Metals* 1986 (Warrendale, PA: TMS-AIME) pp. 885-899.
- [11] D.W. McKee and D. Chatterji, "The Catalytic Behaviour of Alkali Metal Carbonates and Oxides in Graphite Oxidation Reactions", *Carbon*, 13 (1975) pp. 381-390.
- [12] D.W. McKee, "The Catalyzed Gasification Reactions of Carbon", *Chem. and Phys. of Carbon*, 16 (1981) pp. 1-118.
- [13] W.F. Fischer and R. Perruchoud, "Factors Influencing the Carboxy- and Air-Reactivity Behaviour of Prebaked Anodes in Hall-Heroult Cells", *Light Metals* 1986, (Warrendale, PA: TMS-AIME) pp. 575-580.
- [14] T. Müftüoğlu and H.A. Oye. Reactivity and electrolytic consumption of anode carbon with various additives / *Light Metals* 1987, pp. 667 -672.
- [15] G.J. Houston and H.A. Oye, "Consumption of Anode Carbon During Aluminium Electrolysis: I-II", *Aluminium*, 61 (1985) pp. 251-254, 346-349.
- [16] J.F. Rakaszawski and W.E. Parker, "The Effect of Group IIIA-VIA Elements and Their Oxides on Graphite Oxidation", *Carbon*, 2 (1964) pp. 53-63.
- [17] P.J. Rhedey, "A Review of Factors Affecting Carbon Anode Consumption in the Electrolytic Production of Aluminium", *Light Metals* 1971, (Warrendale, PA: TMS-AIME) pp. 385-408.
- [18] A.P. Ratvik et al., "Studies of Composite Anodes for the Production of Aluminium and Magnesium", *Ext. Abstr. Electrochem. Soc. Fall Meeting*, (1985) pp. 736-737.
- [19] T.R. Beck, J.C. Withers and R.O. Loufty, "Composite - Anode Aluminium Reduction Cell", *Light Metals* 1986, (Warrendale, PA: TMS-AIME) pp. 261-266.
- [20] J.F. Rey Boero, *Light Metals* 1981, Proceedings of Sessions, 110th AIME Annual Meeting, Chicago, Illinois, 1981, p.44.
- [21] Tajanchin A.S., Kravcova E.D. Prognozirovanie glubiny zapolneniya pekomo otkrytyh por koksa pri poluchenii anodnoj massy / Sb. dokl. III mezhd. kong. Cvetnye metally, Krasnojarsk, 2011. – pp. 244 – 277.
- [22] Shahraj S. G., Korostovenko V. V., Baranov A.N. Ul'trazvuk. Vozmozhnosti i perspektivy primeneniya v aljuminievoj promyshlennosti. - Cvetnye metally. – №8. – 2010. pp. 43 – 47.
- [23] Lapaev I.I., Shahraj S.G., Sharypov N.A. Sposob proizvodstva anodnoj massy. Patent RF №2464360, Opubl. 20.10.2012., bjul. №29.
- [24] Shahraj S.G., Sharypov N.A., Beljanin A.V. Povyshenie jeffektivnosti propitki koksa pekomo pri proizvodstve anodnoj massy dlja aljuminievyh jelektrolizerov / *Metallurg* - №11. - 2014 g. – pp. 115-117.
- [25] S. Wilkening. Reflections on the Carbon consumption of prebaked anodes. *Light Metals*, 1995, pp. 623–632.
- [26] Shahraj S.G., Poljakov P.V., Mihalev Ju.G. i [dr.]. Sposob zashhity obozhzhennogo anoda aljuminievogo jelektrolizera. Zajavka na izobretenie №2015148448 ot 10.11.2015, reshenie o vydache patenta ot 20.01.2017.
- [27] Shahraj S.G., Poljakov P.V., Skuratov A. P. Sposob ukrytija anodnogo massiva. Patent RF №2586184, opubl. 10.06.2016, bjul. №16.
- [28] Kondratev V.V., Rzhchitsky E.P., Gorovoi V.O., Shakhrai S.G., Karlina A.I. Review of methods of waste lining processing from aluminum electrolyzers // *International Journal of Applied Engineering Research*. 2016. T. 11. № 23. pp. 11374-11381.
- [29] Kondrat'ev V.V., Ershov V.A., Shakhrai S.G., Ivanov N.A., Karlina A.I. Formation and utilization of nanostructures based on carbon during primary aluminum production // *Metallurgist*. 2016. T. 60. № 7-8. pp. 877-882.
- [30] Sysoev I.A., Kondrat'ev V.V., Shahraj S.G., Karlina A.I. Development of the method of electrolyzers' energy mode control for aluminium production // *Tsvetnye metally*. 2016. № 5 (881). pp. 38-43.

- [31] Shahraj S.G., Skuratov A.P., Kondrat'ev V.V., Ershov V.A. Heat recovery of anode gases of aluminium electrolyzer // *Tsvetnye metally*. 2016. № 2 (878). pp. 52-56.
- [32] Kondrat'ev V., Govorkov A., Lavrent'eva M., Sysoev I., Karlina A.I. Description of the heat exchanger unit construction, created in IRNITU // *International Journal of Applied Engineering Research*. 2016. T. 11. № 19. pp. 9979-9983.
- [33] Baranov A.N., Kondratiev V.V., Ershov V.A., Judin A.N., Yanchenko N.I. Improving the efficiency of aluminium production by application of composite chrome plating on the anode pins // *International Journal of Applied Engineering Research*. 2016. T. 11. № 22. pp. 10907-10911.
- [34] Sysoev, I.A., Kondratev, V.V., Kolmogortsev, I.V., Zimina, T.I. Development of heat exchanging tool for recuperation of heat during aluminium production // *Tsvetnye metally*. 2017. № 7. pp. 55-61.
- [35] Shakhrai S.G., Nemchinova N.V., Kondrat'ev V.V., Mazurenko V.V., Shcheglov E.L. Engineering solutions for cooling aluminum electrolyzer exhaust gases // *Metallurgist*. 2017. pp. 1-5.
- [36] Kondrat'ev V.V., Rzhchitskiy E.P., Shakhrai S.G., Karlina A.I., Sysoev I.A. Recycling of electrolyzer spent carbon-graphite lining with aluminum fluoride regeneration // *Metallurgist*. 2016. T. 60. № 5-6. pp. 571-575.
- [37] Rzhchitskiy, E.P., Kondratev, V.V., Karlina, A.I., Shakhrai, S.G. Aluminium fluoride obtaining from aluminium production wastes // *Tsvetnye metally*. 2016. № 4. pp. 23-26.
- [38] Shakhrai S.G., Gron V.A., Kondrat'Ev V.V., Nikolaev V.N., Belyanin A.V. Cooling of the anode gases of aluminum reduction cells in alumina-heating heat exchangers // *Metallurgist*. 2015. T. 59. № 1-2. pp. 126-130.
- [39] Kondrat'Ev V.V., Nemchinova N.V., Ivanov N.A., Ershov V.A., Sysoev I.A. New production solutions for processing silicon and aluminum production waste // *Metallurgist*. 2013. T. 57. № 5-6. pp. 455-459.
- [40] Shakhrai S.G., Sharapov N.A., Mikhalev U.G., Kondrat'ev V.V. and Karlina A.I. Quality of anode. Overview of Problems and Some Methods of their Solution Part 1. Coal Foam in an aluminum electrolyzer // *International Journal of Applied Engineering Research*. 2017. T. 12. № 19. pp. 8976-8985.